Room-Temperature Quantum Sensing in CMOS: On-Chip Detection of Electronic Spin States in Diamond Color Centers for Magnetometry

Mohamed I. Ibrahim[†*], Christopher Foy[†], Donggyu Kim[†], Dirk R. Englund, and Ruonan Han

Massachusetts Institute of Technology, Cambridge, MA, 02139, USA *E-mail: ibrahimm@mit.edu

Abstract

In this paper, we report the first on-chip quantum sensor that combines compact and multifunctional CMOS integrated circuit technologies with nitrogen-vacancy (NV) centers in diamond. The system performs two critical functions for quantum magnetometry with NV centers: strong generation and efficient delivery of microwave for quantum-state control, and optical filtering/detection of spin-dependent fluorescence for quantum-state readout. In particular, we experimentally demonstrate on-chip optically detectable magnetic resonance (ODMR) for the first time.

Keywords: CMOS, nitrogen vacancy, quantum, magnetometer

Introduction

Room-temperature sensors based on quantum coherence are gaining increased attention. For instance, NV centers (Fig. 1), consisting of a nitrogen atom and a vacancy that substitute an adjacent pair of carbon atoms in the diamond lattice, have been extensively exploited in recent years for magnetic field sensing [1,2] and imaging [3] with a high sensitivity under ambient conditions. However, existing NV-based sensing platforms [1-3] involve bulky and discrete instruments to control and measure spin states, which makes them impractical and difficult to scale up for advanced quantum-enhanced sensing protocol [4]. To address this challenge, we report for the first time, a single-chip spin-control/detection system using standard CMOS process. ODMR is the key for NV-based quantum magnetometry, in which the magnetic resonance between the spin sub-levels m_s=0 and ±1 is optically detected through spin-dependent fluorescence. By applying a microwave (f_0=~2.87GHz) and measuring the fluorescence emission (I_f) of the NV under green-light excitation, the magnetic resonance is shown as a dip in the f_0-I_f plot (i.e. ODMR spectrum as shown in Fig. 1 (right)). Since an external magnetic field shifts the resonance frequencies f_0 of ±1 spin states by Zeeman effect ($\Delta f_0 = \pm g\mu_B B_z/h$, where $g \approx 2$ is the gyromagnetic ratio, μ_B is Bohr magneton, h is Boltzmann constant, and B_z is the projection of the external magnetic field along the N-V direction), the value of B_z is then determined by the measured f_0 of the ODMR spectrum. Through a tightly-integrated microwave launcher, photonic filter and sensor, the CMOS circuit of this work provides direct physical interactions with the quantum states and generates the ODMR. The role of CMOS circuits in a quantum system therefore goes beyond electronic I/O signaling [5], and enables ultra-compact and highly-scalable platforms for quantum sensing and potentially information processing under cryogenic condition.

Design of the On-Chip Quantum Sensing System

In this section, we describe the implementations of a spin excitation/detection sub-system, which is the key of a complete sensing platform shown in Fig. 2. The platform is a feedback loop, where the output frequency f_{res} is locked to one (or both) of the split ODMR resonance frequencies (similar to the electronics in atomic clocks), and is then used to calculate the applied magnetic field strength. For the efficient excitation of the m_s= ±1 spin states under optical pumping, we apply 10Gauss AC magnetic field around the resonance frequency (2.87GHz). Previously, this was achieved by external coils or wires driven by large AC current. Thanks to the close proximity between the chip and the NV centers, per Ampere's Law, such field strength becomes possible by an on-chip multi-loop coil driven at a current level that is deliverable by an on-chip ring VCO and driver. Meanwhile, a pair of shunt capacitors is added to form resonance near 2.87GHz; the AC magnetic field is therefore amplified by a factor Q with the same driver current (~5mA), where Q (~15) is the quality factor of coil (Fig. 3 (left)). It is also noteworthy that high uniformity of magnetic field across the coil-enclosed region is desired to minimize inhomogeneous broadening of ODMR spectrum. To this end, a set of broken parasitic loops (Fig. 3 (right)) are inserted: the magnetic field generated by the induction currents in these capacitively-coupled loop sections counteracts the field from the main loop at the loop edge, thus improving the overall field uniformity to >95% (Fig. 3).

To optically detect the NV-emitted red fluorescence, an on-chip p+/n-well photodiode is placed inside the coil. Two critical challenges are addressed: first, since the photodiode consists of conductive silicon layers, large eddy current near 2.87GHz is induced by the coil above and in turn leads to large loss and Q (hence magnetic field strength) reduction of the coil. Our analysis shows that for square photodiode with dimension of $L \times L$, such power loss is proportional to L^3. Therefore, we adopt a device pattern where the active layer is split into four parts (Fig. 4). The eddy current is therefore cut by the shallow-trench isolation (STI) between the parts, and the total loss is reduced by $L^3/[4\cdot(L/2)^3]=2\times$. This is similar to the patterned ground shield used in on-chip inductor designs [6]. Anode/cathode interconnects are also placed with a radial pattern so that eddy current flow cannot be formed. The measured responsivity of the photodiode is 0.23A/W. The second challenge of on-chip fluorescence detection is the presence of green light with high intensity (532nm) applied externally as optical pump. It significantly lowers the contrast and increases shot noise of the measured ODMR. To filter the green light, an integrated optical filter consisting of a periodic grating structure in M8 layer is used (Fig. 5). With a metal spacing of 400nm, the filter provides ~10dB green-light suppression by coupling the incident laser into a lossy surface plasmon polariton mode. In contrast, photons of spin-dependent red fluorescence pass through the M8 layer with a transmission rate of 0.96. With a finite-difference time-domain (FDTD) method, simulated field profiles at the wavelengths of 532nm (green) and 700nm (red) are shown in Fig. 5 (right).

Measurement Results

A chip prototype (Fig. 6) is implemented using a 65nm bulk CMOS technology. To deposit the diamond nanocrystals with NV ensembles on the chip, first, the chip passivation layer, which emits unwanted background red fluorescence in our

testing, is etched using CF_4 plasma. Next, a drop of nano-diamond solution is applied on the treated chip surface; nanodiamond is then attached to the chip via van der Waals' force after drying (Fig. 6 (right)). Figure 7 shows a green-laser-pumped test setup using external optical detection. By sweeping the on-chip microwave frequency, an ODMR spectrum with a contrast of 10% is successfully obtained. Next, another setup with on-chip optical detection is shown in Fig. 8, The microwave signal is AM modulated (f_m=1kHz), so in the fluorescence-induced current, only the component caused by ±1 spins has a frequency of f_m. This current component is then measured by a lock-in amplifiers and generates the ODMR in Fig. 8. In both cases, when an external static magnetic field is applied, Zeeman effect is observed. Since the crystal orientation of nanodiamond is random, the effective B_z (hence the amount of splitting) for each orientation varies. As a result, spectral broadening, rather than splitting, is observed. Replacement of nanodiamond with single-crystal diamond addresses this issue. To the authors' best knowledge, this is the first demonstration of CMOS-integrated quantum sensing.

†*These authors made equal contribution to this work.*

References

[1] G. Balasubramanian, et al. *Nature*, pp. 648-651, Oct. 2008.
[2] H. Clevenson, et al., *Nature Physics*, pp. 393-397, May 2015
[3] Le Sage, et al. *Nature,* pp. 486–489, April 2013
[4] V. Giovannetti, et al., *Nature photonics*, pp.222, April 2011.
[5] E. Charbon, et al., *ISSCC*, Feb. 2017.
[6] Thomas H. Lee, Cambridge University Press, 2nd Edition, 2004.

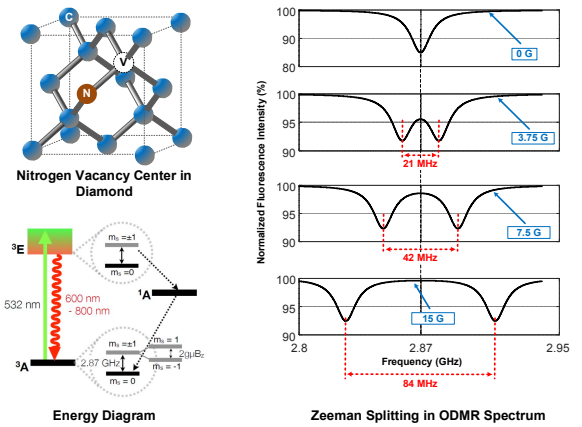

Fig. 1 The lattice structure and energy levels of nitrogen vacancy center in diamond (left) and the fluorescence intensity of NV centers, stimulated at various external magnetic field strengths (right).

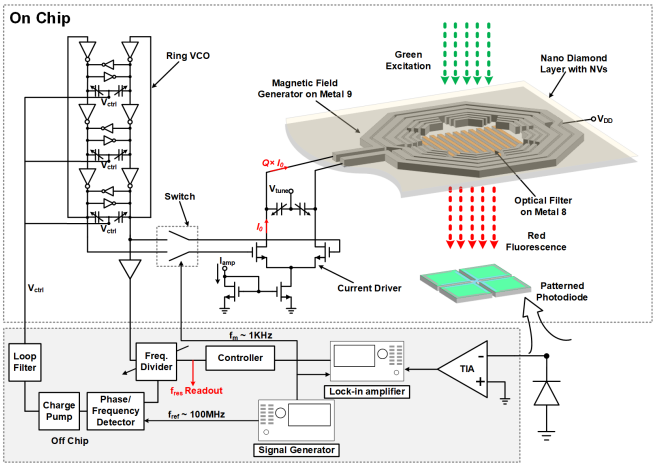

Fig. 2 Circuit schematic of the NV-based magnetic sensor using a 65nm CMOS technology.

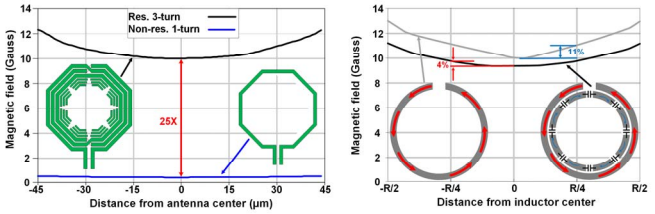

Fig. 3 The simulated magnetic field profiles of the proposed resonant inductor and a non-resonant one (left), and the simulated magnetic field profiles of inductors with and without capacitive loop (right).

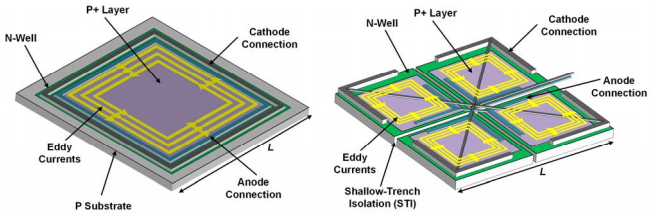

Fig. 4 Schematics of a conventional photodiode (left) and the adopted patterned photodiode (right).

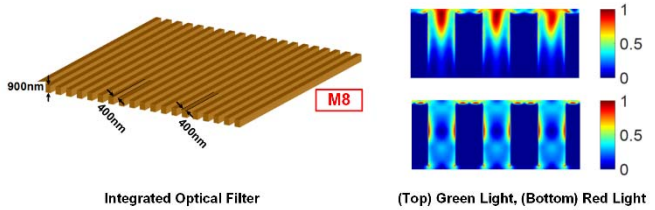

Fig. 5 Schematic of the optical filter (left), and simulated light transmission of the filter (right).

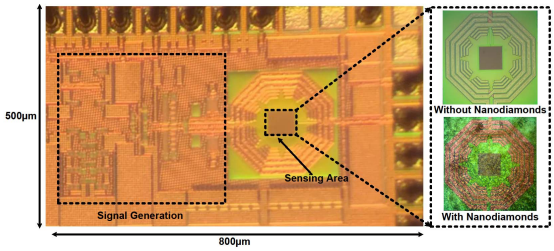

Fig. 6 Chip photo and the area with/without nanodiamonds.

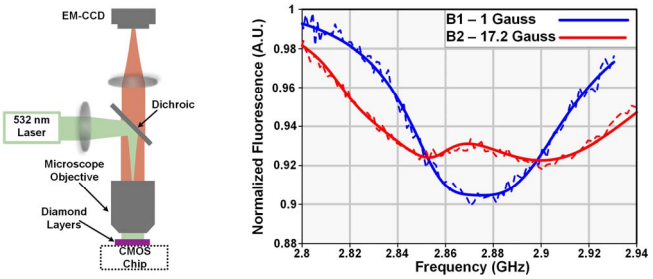

Fig. 7 Test setup using off-chip camera (left), and measured and fitted ODMR spectrum using off-chip camera (right).

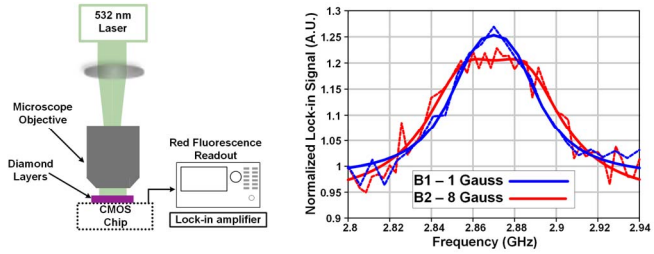

Fig. 8 Test setup using on-chip photodiode (left), and measured and fitted ODMR spectrum using on-chip photodiode (right).